



PII: S0017-9310(96)00209-8

Film condensation induced by a natural convective flow: steady-state analysis

F. MÉNDEZ

Facultad de Ingeniería, UNAM, 04510 México D. F., Mexico

and

C. TREVIÑO†

Facultad de Ciencias, UNAM, 04510 México D. F. Mexico

(Received 5 February 1996 and in final form 3 June 1996)

Abstract—In this paper we study the laminar condensation process of a saturated vapor in contact with one side of a vertical thin plate, caused by a natural laminar boundary layer flow on the other surface of the plate. The effects of both longitudinal and transversal heat conduction in the plate are considered. The momentum and energy balance equations are reduced to a system of differential equations with five parameters. Asymptotic and numerical solutions for the temperature and condensed film thickness distributions are presented for all possible values of the nondimensional plate thermal conductance α .

Copyright © 1996 Elsevier Science Ltd.

1. INTRODUCTION

Due to its fundamental and practical importance, we consider here the conjugate coupling heat transfer between a condensation process of a saturated vapor in contact with a surface of a vertical plate, caused by a natural convection flow on the other surface of the plate. The importance of solid heat conduction associated with natural convection in boundary layer flows is well known. Conjugate heat transfer configurations have been studied using different approximations. However, the theoretical studies of film condensation processes with non-isothermal wall conditions have received little attention in the literature.

Patankar and Sparrow [1] solved the problem of condensation on an extended surface by considering the heat conduction in a fin coupled with the condensation process. Their numerical solution of the governing equations confirms the influence of non-isothermal extended surface over the condensing process. Wilkins [2] showed that an explicit analytical solution is possible for the formulation of Patankar and Sparrow. Sarma *et al.* [3] studied the condensation process on a vertical plate fin of variable thickness. They studied the effect of the fin geometry on the condensation heat transfer and found that this interaction is very important. Brouwers [4] performed an analysis of the condensation of a pure saturated vapor on a cooled channel plate, including the interaction between the cooling liquid, the condensate and

the vapor. He obtained in closed form the solution of the governing equations, confirming that this interaction has to be taken into account in order to have more realistic models for this type of process. Méndez and Treviño [5] analyzed the film condensation process of a saturated vapor in contact with one side of a vertical plate, caused by a forced flow on the other side of the plate. They showed that effects of the heat conduction through the plate substantially modify the classical Nusselt's solution [6].

Recently Treviño and Méndez [7] studied the transient conjugate condensation process on one side of a vertical plate, caused by a uniform cooling rate on the other surface of the plate, including the finite thermal inertia. In this work, the transient evolution of the condensed layer thickness and the temperature of the plate were obtained using different realistic limits, including the cases of very good and poor conducting plates. Their main results obtained indicated that the condensed layer thickness evolution is almost insensitive to the longitudinal heat conduction effects through the plate, for a thermally thin plate and that the wall thermal inertia was the controlling factor for the transient condensation process, in most practical cases.

We present in this paper a theoretical analysis of the film condensation process on one lateral surface of a vertical flat plate produced by a cooling natural flow on the other lateral surface of the plate. For simplicity we assume the vapor to be saturated. This condensation process can be characterized mainly by three nondimensional parameters α , ε and β . Parameter α represents the competition between the heat

† Author to whom correspondence should be addressed.

NOMENCLATURE

c_f	specific heat of the cooling fluid	ε	aspect ratio of the plate, $\varepsilon = h/L$
c_c	specific heat of the condensed phase	γ	nondimensional parameter defined in equation (3)
f_c	nondimensional stream function introduced in equation (22)	λ_c	thermal conductivity of the condensed phase
f_F	nondimensional stream function for the cooling fluid	λ_F	thermal conductivity of the cooling fluid
g	acceleration of gravity	λ_w	plate thermal conductivity
h	thickness of the plate	μ_c	dynamic viscosity of the condensed fluid
h_{ig}	latent heat of condensation	η_c	nondimensional transversal coordinate for the condensed fluid flow
Ja	Jakob number defined in equation (4)	η_F	nondimensional transversal coordinate for the cooling fluid flow
L	length of the plate	ρ_c	condensed fluid density
m'	mass flow rate of condensed fluid	ρ_F	cooling fluid density
Nu_c	Nusselt number	θ_c	nondimensional temperature of the condensed layer
Pr_F	Prandtl number of the cooling fluid	θ_F	nondimensional temperature of the cooling fluid
Pr_c	Prandtl number of the condensed fluid	θ_w	nondimensional temperature of the plate
Ra	Rayleigh number of the cooling natural convective fluid flow	v_c	kinematic coefficient of viscosity of the condensed fluid
T	temperature	v_F	kinematic coefficient of viscosity of the cooling fluid
T_∞	ambient temperature of the cooling fluid	χ	nondimensional longitudinal coordinate defined in equation (19).
T_s	temperature of the saturated vapor		
T_F	temperature of the cooling fluid		
\bar{u}, \bar{v}	longitudinal and transversal velocities in physical units		
u, v	nondimensional longitudinal and transversal velocities		
u_c	characteristic longitudinal velocity of the condensed fluid		
x, y	Cartesian coordinates.		

Greek symbols		Subscripts	
α	heat conduction parameter defined in equation (10)	c	refers to the condensed fluid
β	nondimensional parameter defined in equation (8)	F	refers to the cooling fluid
Δ	normalized thickness of the condensed layer	L	conditions at the leading edge of the wall
δ_c	thickness of the condensed layer	l	conditions at the trailing edge of the wall
δ_F	thickness of the cooling flow layer	w	conditions at the wall.

flux conducted longitudinally through the plate with the heat flux transferred into the plate from the condensed phase. The aspect ratio of the plate is denoted by ε and β defines the ratio of the thermal resistance of the cooling natural flow to the thermal resistance of the condensed fluid. We also present an asymptotic analysis for large and small values of α compared with unity, assuming finite values of β and values of ε which are very small compared with unity. Finally we compare the analytical solutions with the results obtained using numerical techniques.

2. ORDER OF MAGNITUDE ESTIMATES

The physical model under study is shown in Fig. 1. The right-side of a thin vertical plate of length L and

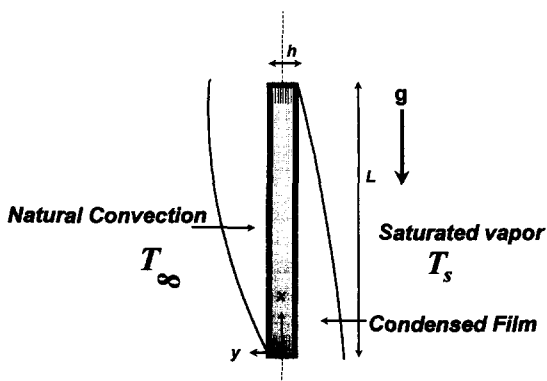


Fig. 1. Schematic diagram of the studied physical model.

thickness h is placed in a stagnant atmosphere filled with saturated vapor with a temperature T_s . A natural convective flow of a cooling fluid with temperature $T_\infty < T_s$ at the left lateral surface of the plate is produced, thus generating a convective heat flux from the saturated vapor and creating a thin condensed film with increasing thickness falling due to gravity at the right lateral surface of the plate. The lower edge of the plate coincides with the origin of a Cartesian coordinate system whose y -axis is the horizontal distance from the middle of the plate and its x -axis is the vertical distance measured from its lower edge, that is in the opposite direction to the gravitational force. An adiabatic wall with the same thickness h , is assumed above the leading edge and below the trailing edge. The density of the condensed fluid, ρ_c , is assumed to be constant and much larger than the vapor density. The inclusion of a finite thermal conductivity of the plate material, enables heat conduction to be measured in both longitudinal and transversal coordinates through the plate. We are interested in obtaining the steady-state solution of this counter-flow configuration, in particular, in the temperature distribution of the plate, the overall heat transfer rate of the plate and the condensed layer thickness distribution.

From the balance of the body to viscous forces in the momentum equation for the condensed fluid in the longitudinal direction x , it can be easily shown that the condensed fluid longitudinal velocity is of the order, $u_c \sim (g/\nu_c)\delta_c^2$, where δ_c is the characteristic condensed layer thickness, g is the acceleration of gravity and ν_c is the kinematic coefficient of viscosity. The condensed mass flow rate, m' is then of the order $m' \sim \rho_c g \delta_c^3 / \nu_c$. The production rate of condensed fluid can be obtained from the thermal energy balance at the condensed-vapor interface as

$$\frac{dm'}{dx} \sim -\frac{\rho_c g \delta_c^2}{\nu_c} \frac{d\delta_c}{dx} \sim \frac{\lambda_c \Delta T_c}{\delta_c h_{lg}} \quad (1)$$

where h_{lg} corresponds to the latent heat of condensation and λ_c represents the thermal conductivity of the condensed phase and ΔT_c is the characteristic transversal temperature change in the condensed phase, estimated below. Therefore, from relationship (1), we can obtain the thickness of the condensed layer related to the length of the plate as

$$\frac{\delta_c}{L} \sim \left(\frac{Ja \Delta T_c}{\gamma \Delta T} \right)^{1/4} \quad (2)$$

Here, γ is a nondimensional still unnamed parameter [8],

$$\gamma = \frac{gL^3}{\nu_c^2} \gg 1 \quad (3)$$

Ja corresponds to the suitable Jakob number and represents the ratio of the sensible heat energy absorbed by the liquid to the latent heat of the liquid during condensation, defined by

$$Ja = \frac{4}{Ku Pr_c} = \frac{4c_c \Delta T}{h_{lg} Pr_c} \quad (4)$$

c_c is the specific heat capacity, Pr_c is the Prandtl number, $Pr_c = \nu_c \rho_c c_c / \lambda_c$, of the condensed fluid, Ku represents the Kutateladse number [9] and $\Delta T = T_s - T_\infty$ represents the temperature difference between the saturated vapor and the cooling fluid. In general, the Jakob number is very small compared with unity [9] and thus we can use the boundary layer approximation for the condensed fluid flow in the limit $Ja/\gamma \rightarrow 0$.

On the other lateral surface of the plate facing the cooling natural convective flow, for fluids with Prandtl of order unity or large, the characteristic thickness of the induced natural convective boundary layer is of order [10]

$$\frac{\delta_F}{L} \sim \left(\frac{1}{Ra} \frac{\Delta T}{\Delta T_F} \right)^{1/4} \quad (5)$$

Here, ΔT_F is the characteristic transversal temperature change in the cooling natural flow, also estimated below and $Ra \gg 1$ is the Rayleigh number defined by [10]

$$Ra = \frac{g \beta_F \Delta T L^3 \rho_F c_F}{\nu_F \lambda_F} \quad (6)$$

where ρ_F , c_F , β_F , ν_F and λ_F are the density, specific heat (at constant pressure for a gas), coefficient of thermal expansion, kinematic coefficient of viscosity and thermal conductivity of the cooling fluid, respectively.

2.1. Estimation of ΔT_w , ΔT_c and ΔT_F

We assume throughout the paper that the aspect ratio of the plate, $\varepsilon = H/L$, is very small compared with unity and also suppose, as mentioned previously, that the upper and lower edges of the plate are adiabatic. In this case, the overall heat fluxes across the film condensation layer, the flat plate and the natural boundary layer, are of the same order of magnitude, that is

$$\lambda_c \frac{\Delta T_c}{\delta_c} \sim \lambda_w \frac{\Delta T_w}{h} \sim \lambda_F \frac{\Delta T_F}{\delta_F} \quad (7)$$

where, λ_w is the thermal conductivity of the plate and ΔT_w is the characteristic transversal temperature change across the plate. If we compare the first and third terms in equation (7) and using equations (2) and (5), we obtain the following relationship between the characteristic temperatures in the condensed phase and the cooling fluid as

$$\frac{\Delta T_c^{3/4} \Delta T^{2/4}}{\Delta T_F^{5/4}} \sim \frac{\lambda_F}{\lambda_c} \left(\frac{Ra Ja}{\gamma} \right)^{1/4} = \beta. \quad (8)$$

Similarly, comparing the first and second terms of equation (7) and using equation (5), we derive the following relationship between the characteristic tem-

perature change in the condensed phase to the overall temperature drop

$$\frac{\Delta T_c}{\Delta T} \sim \left(\frac{\alpha}{\varepsilon^2} \right)^{4/3} \left(\frac{\Delta T_w}{\Delta T} \right)^{4/3} \quad (9)$$

where α is the heat conduction parameter defined by

$$\alpha = \frac{\lambda_w h \left(\frac{Ja}{\gamma} \right)^{1/4}}{\lambda_c L}. \quad (10)$$

Condensing equation (9) into equation (8), we obtain also

$$\frac{\Delta T_F}{\Delta T} \sim \left(\frac{\alpha}{\beta \varepsilon^2} \right)^{4/5} \left(\frac{\Delta T_w}{\Delta T} \right)^{4/5}. \quad (11)$$

Parameter α relates the competition between the heat conducted longitudinally by the plate to the heat convected from the condensed-vapor fluid. For $\alpha \gg 1$, the heat conducted by the plate is very large, thus no temperature gradients of importance arise in the longitudinal direction. On the other hand, for $\alpha \ll 1$, the heat convected from the condensed fluid is extremely important, the longitudinal heat conduction is then weak and large longitudinal temperature gradients arise on the plate. Using equations (9) and (11) and noting that $\Delta T_F + \Delta T_w + \Delta T_c \sim \Delta T$, we obtain the following relationship for ΔT_w

$$\left(\frac{\alpha}{\beta \varepsilon^2} \right)^{4/5} \left(\frac{\Delta T_w}{\Delta T} \right)^{4/5} \left[1 + \beta^{4/5} \left(\frac{\alpha}{\varepsilon^2} \right)^{8/15} \left(\frac{\Delta T_w}{\Delta T} \right)^{8/15} \right] + \frac{\Delta T_w}{\Delta T} \sim 1. \quad (12)$$

In the following section, we define the distinguishable limits depending on the assumed asymptotic values of α/ε^2 and β .

2.2. Relevant limits for the thermally thin case ($\alpha/\varepsilon^2 \gg 1$)

In this limit, the transversal variations of the temperature in the plate, ΔT_w , are very small compared with the overall temperature difference, ΔT , representing the thermally thin wall approximation. We consider three possibilities: $\beta \gg 1$, $\beta \sim 1$ and $\beta \ll 1$. In the first, the second term of the left-hand side of equation (12) is much larger than the first term, giving, with the aid of equations (9) and (11), in a first approximation

$$\frac{\Delta T_w}{\Delta T} \sim \frac{\varepsilon^2}{\alpha}, \quad \frac{\Delta T_c}{\Delta T} \sim 1, \quad \frac{\Delta T_F}{\Delta T} \sim \beta^{-4/5}. \quad (13)$$

Here, the nondimensional transversal temperature variations in the solid are very small, of order ε^2/α at most and the temperature of the plate practically assumes the value of the temperature of the cooling flow T_∞ . This represents the well-known classical Nusselt's solution for the film condensation process and

can be found elsewhere [6, 11]. In the second case, with $\beta \sim 1$, we obtain

$$\frac{\Delta T_w}{\Delta T} \sim \frac{\varepsilon^2}{\alpha}, \quad \frac{\Delta T_c}{\Delta T} \sim 1, \quad \frac{\Delta T_F}{\Delta T} \sim 1. \quad (14)$$

Here, although the nondimensional transversal temperature variations in the solid are very small, of order ε^2/α , the characteristic nondimensional temperatures at both the condensed and the cooling fluids are significant, causing variations in the longitudinal temperature of the plate.

For the last option, with $\beta \ll 1$, we obtain

$$\frac{\Delta T_w}{\Delta T} \sim \frac{\beta \varepsilon^2}{\alpha}, \quad \frac{\Delta T_c}{\Delta T} \sim \beta^{4/3}, \quad \frac{\Delta T_F}{\Delta T} \sim 1. \quad (15)$$

In this case, the temperature of the right-hand side of the plate is practically the saturated vapor temperature T_s . Therefore the condensation process is inhibited because the characteristic temperature change in the cooling fluid is now relevant and thus the classical case of a natural boundary layer flow on the left hand side of the plate subject at a uniform temperature T_s , is developed. In this case the solution is widely known [8].

2.3. Relevant limits for the thermally thick case ($\alpha/\varepsilon^2 \sim 1$)

Proceeding in a similar form as the above subsection, in this limit the transversal temperature drop in the solid is very important. This corresponds to the thermally thick wall approximation. In this asymptotic limit for values of $\beta \gg 1$, we obtain

$$\frac{\Delta T_w}{\Delta T} \sim 1, \quad \frac{\Delta T_c}{\Delta T} \sim 1, \quad \frac{\Delta T_F}{\Delta T} \sim \beta^{-4/5}. \quad (16)$$

Here, the temperature of the coolant side of the plate is practically T_∞ and the film condensation process is governed by the unknown temperature variations on the plate, which are dictated by the heat conduction equation in solid. However, for $\beta \sim 1$, the equivalent relationship for this case assumes the form

$$\frac{\Delta T_w}{\Delta T} \sim 1, \quad \frac{\Delta T_c}{\Delta T} \sim 1, \quad \frac{\Delta T_F}{\Delta T} \sim 1 \quad (17)$$

that is, the global characteristic temperature changes are all important and it has a big influence over the condensation process. Finally, for $\beta \ll 1$, we have

$$\frac{\Delta T_w}{\Delta T} \sim \beta^{4/5}, \quad \frac{\Delta T_c}{\Delta T} \sim \beta^{1/15}, \quad \frac{\Delta T_F}{\Delta T} \sim 1 \quad (18)$$

reproducing again the classical natural boundary layer flow. We know that values of $\alpha/\varepsilon^2 \ll 1$ lead to the pure conducting plate being influenced by weak condensing and natural boundary layer flow processes.

3. FORMULATION

Following the order of magnitude analysis, we introduce the following nondimensional variables

$$\begin{aligned}\theta_w &= \frac{T_w - T_\infty}{T_s - T_\infty} & \chi &= \frac{x}{L} & \tilde{\chi} &= \frac{L-x}{L} \\ \theta_c &= \frac{T_c - T_\infty}{T_s - T_\infty} & \theta &= \frac{T_F - T_\infty}{T_s - T_\infty} & z &= \frac{y}{h} \\ \eta_c &= -\frac{(y+h/2)}{\delta_c} & \eta_F &= \frac{Ra^{1/4}(y-h/2)}{L\chi^{1/4}} & \Delta &= \frac{\delta_c}{\delta_{cl}}\end{aligned}\quad (19)$$

where $\delta_{cl} = L(Ja/\gamma)^{1/4}$ and the subscript L refers to the condition at the upper edge of the plate, $\chi = 1$ (or $\tilde{\chi} = 0$). The variables with subscript c denote the variables of the condensed phase, w denotes the variables in the wall and subscript F represents the variables of the cooling fluid. δ_c is the thickness of the condensed flow and similarly, δ_F corresponds to the thickness of the laminar boundary layer of the cooling fluid. The Laplace equation describing the heat conduction in the solid is

$$\frac{\partial^2 \theta_w}{\partial \chi^2} + \frac{1}{\varepsilon^2} \frac{\partial^2 \theta_w}{\partial z^2} = 0. \quad (20)$$

Assuming, for simplicity, the two edges of the plate to be adiabatic, the boundary conditions needed to solve equation (20) are given by

$$\frac{\partial \theta_w}{\partial \chi} = 0 \quad \text{at } \chi = 0 \quad \text{and} \quad \chi = 1. \quad (21)$$

We also introduce the nondimensional stream function f_c for the condensed fluid as

$$\begin{aligned}u_c &= \frac{\bar{u}_c}{\sqrt{gLJa}} = \Delta^2 \frac{\partial f_c}{\partial \eta_c} \\ v_c &= \frac{\bar{v}_c \gamma^{1/4}}{Ja^{3/4} \sqrt{gL}} = -\Delta \frac{\partial(\Delta^2 f_c)}{\partial \tilde{\chi}}\end{aligned}\quad (22)$$

where \bar{u}_c and \bar{v}_c represent the longitudinal and transverse velocity components in physical units. On the other hand, for the laminar cooling fluid flow, we can define the following dimensionless variable

$$f_F(\chi, \eta_F) = \frac{\Psi_F}{v_F Ra^{1/4} \chi^{3/4}} \quad (23)$$

for the upward moving fluid in the boundary layer at the left of the plate. Here, f_F and Ψ_F are the non-dimensional and dimensional scaled stream functions of the cooling fluid flow, respectively. The momentum and energy balance equations for the condensed fluid, using the boundary layer approximation, take the form

$$\begin{aligned}\frac{\partial^3 f_c}{\partial \eta_c^3} + 1 &= Ja \Delta^4 \left\{ \frac{\partial f_c}{\partial \eta_c} \frac{\partial^2 f_c}{\partial \tilde{\chi} \partial \eta_c} - \frac{\partial f_c}{\partial \tilde{\chi}} \frac{\partial^2 f_c}{\partial \eta_c^2} \right. \\ &\quad \left. + \frac{2}{\Delta} \frac{d\Delta}{d\tilde{\chi}} \left(\left(\frac{\partial f_c}{\partial \eta_c} \right)^2 - f_c \frac{\partial^2 f_c}{\partial \eta_c^2} \right) \right\} \quad (24)\end{aligned}$$

$$\begin{aligned}\frac{\partial^2 \theta_c}{\partial \eta_c^2} &= Ja Pr_c \Delta^4 \left\{ \frac{\partial f_c}{\partial \eta_c} \frac{\partial \theta_c}{\partial \tilde{\chi}} \right. \\ &\quad \left. - \frac{\partial f_c}{\partial \tilde{\chi}} \frac{\partial \theta_c}{\partial \eta_c} - \frac{2}{\Delta} \frac{d\Delta}{d\tilde{\chi}} f_c \frac{\partial \theta_c}{\partial \eta_c} \right\} \quad (25)\end{aligned}$$

with the boundary conditions

$$f_c = \frac{\partial f_c}{\partial \eta_c} = 0 \quad \text{at } \eta_c = 0 \quad (26)$$

$$\theta_c - 1 = \frac{\partial^2 f_c}{\partial \eta_c^2} = 0 \quad \text{at } \eta_c = 1. \quad (27)$$

The second condition of equation (27) arises from the balance of tangential shear stress at the interface. The normalized nondimensional thickness of the condensed film Δ is unknown and must be obtained from the analysis. The energy balance at the condensed-vapor interface gives the evolution of Δ as

$$4\Delta \frac{d(\Delta^3 f_c(\chi, 1))}{d\tilde{\chi}} = \frac{\partial \theta_c}{\partial \eta_c} \Big|_{\eta_c=1}. \quad (28)$$

The initial condition for equation (28) is given by $\Delta(\tilde{\chi} = 0) = 0$.

Similarly using the boundary layer approximation, the momentum and energy equations for the cooling fluid can be written as:

$$\begin{aligned}\frac{\partial^3 f_F}{\partial \eta_F^3} + \theta_F &= \frac{1}{Pr_F} \left\{ \frac{1}{2} \left(\frac{\partial f_F}{\partial \eta_F} \right)^2 - \frac{3}{4} f_F \frac{\partial^2 f_F}{\partial \eta_F^2} \right. \\ &\quad \left. + \chi \left[\frac{\partial f_F}{\partial \eta_F} \frac{\partial^2 f_F}{\partial \chi \partial \eta_F} - \frac{\partial f_F}{\partial \chi} \frac{\partial^2 f_F}{\partial \eta_F^2} \right] \right\} \quad (29)\end{aligned}$$

$$\frac{\partial^2 \theta_F}{\partial \eta_F^2} = -\frac{3}{4} f_F \frac{\partial \theta_F}{\partial \eta_F} + \chi \left[\frac{\partial f_F}{\partial \eta_F} \frac{\partial \theta_F}{\partial \chi} - \frac{\partial f_F}{\partial \chi} \frac{\partial \theta_F}{\partial \eta_F} \right] \quad (30)$$

with the boundary conditions

$$f_F = \frac{\partial f_F}{\partial \eta_F} = 0 \quad \text{at } \eta_F = 0 \quad (31)$$

$$\theta_F = \frac{\partial f_F}{\partial \eta_F} = 0 \quad \text{for } \eta_F \rightarrow \infty. \quad (32)$$

At the interfaces of the solid-coolant and solid-condensed phase ($z = \pm 1/2$), continuity of the temperature and the heat flux gives

$$\theta_F(\chi, \eta_F = 0) = \theta_w(\chi, z = 1/2)$$

$$\text{and} \quad \frac{\partial \theta_w}{\partial z} \Big|_{z=1/2} = \frac{\varepsilon^2 \beta}{\alpha} \frac{1}{\chi^{1/4}} \frac{\partial \theta_F}{\partial \eta_F} \Big|_{\eta_F=0} \quad (33)$$

and

$$\theta_c(\tilde{\chi}, \eta_c = 0) = \theta_w(\tilde{\chi}, z = -1/2)$$

$$\text{and } \left. \frac{\partial \theta_w}{\partial z} \right|_{z=-1/2} = -\frac{\varepsilon^2}{\alpha} \frac{1}{\Delta} \left. \frac{\partial \theta_c}{\partial \eta_c} \right|_{\eta_c=0} \quad (34)$$

The solution of equations (20)–(34) should provide the following functional relationship:

$$\theta_w = \mathcal{F}(\alpha, \beta, \varepsilon, Pr_F, Pr_c, \chi, z).$$

In the following sections we analyze the relevant limits characterized by small Jakob numbers, $Ja \rightarrow 0$, with both Prandtl numbers of order unity. In this limit, we classify the solutions according to the value of α , taking advantage of the fact that ε^2 is very small, in general. For large values of α/ε^2 (thermally thin walls) the nondimensional transversal temperature variations in the plate are very small and the plate temperature can only be assumed as a function of the longitudinal coordinate χ . It should be noted that neglecting the transversal temperature variations doesn't mean neglecting the transversal temperature gradient, which is always retained in the analysis. We analyze the limit of large values of α using perturbation techniques. In the other limit of α/ε^2 of order unity (thermally thick wall), the temperature variations across the plate must be taken into account, but the longitudinal heat conduction is then negligible, except in small regions close to the edges of the plate. Numerical solutions for all possible values of α are presented and the asymptotic limits for small values of α/ε^2 are also analyzed.

4. ASYMPTOTIC SOLUTION FOR $Ja \rightarrow 0$

The governing equations (24)–(27) for the condensed fluid simplify, giving a linear profile for the temperature and a cubic profile for f_c as

$$\theta_c = \theta_w(\chi) + [1 - \theta_w(\chi)]\eta_c$$

$$\text{and } f_c(\eta_c) = \frac{1}{2}\eta_c^2 \left(1 - \frac{\eta_c}{3}\right). \quad (35)$$

The appropriate or reduced Nusselt number for this problem Nu_c^* is given by

$$Nu_c^* = Nu_c \left(\frac{Ja}{\gamma}\right)^{1/4} = \frac{1}{\Delta} \left. \frac{\partial \theta_c}{\partial \eta_c} \right|_{\eta_c=0} = \frac{1 - \theta_w}{\Delta} \quad (36)$$

where the nondimensional heat flux (local Nusselt number) is defined by

$$Nu_c = \left| \frac{qL}{\lambda_c(T_s - T_\infty)} \right|$$

where q is the local heat flux from the condensed fluid to the plate. Thus, the nondimensional energy balance equation (28) at the interface of the vapor-condensed fluid transforms to

$$\frac{d\Delta^4}{d\tilde{\chi}} = 1 - \theta_w \quad (37)$$

to be solved with the initial condition $\Delta(0) = 0$.

4.1. Limit $\varepsilon \rightarrow 0$ with α finite (thermally thin wall)

In this case the nondimensional transversal temperature variations in the plate are very small, of order ε^2/α . Here, the governing equations (20), (21), together with equations (29)–(34) and (37), have been solved numerically for all values of α . For this purpose, the nondimensional wall temperature θ_w was computed, from equations (20) and (21), by using a pseudo-transient procedure, rewriting equation (20) in the form

$$\frac{\partial \theta_w}{\partial \tau} = \frac{\partial^2 \theta_w}{\partial \chi^2} + \frac{1}{\varepsilon^2} \frac{\partial^2 \theta_w}{\partial z^2} \quad (38)$$

and marching in the artificial time τ . At $\tau = 0$, we suppose an arbitrary profile of θ_w , which is used to solve equations (29)–(34) until a steady state is achieved. Later, we calculate equation (38) subject to equations (21), (33) and (34), in order to obtain a new profile of θ_w , and the iteration is repeated for a new value of τ . In Section 5, we present the numerical results for different values of the parametric set.

4.1.1. *Asymptotic limit $\alpha \rightarrow \infty$.* Integrating the energy equation (20) transversely across the solid and applying the boundary conditions (33) and (34), we obtain

$$\alpha \frac{d^2 \theta_w}{d\chi^2} + \frac{1}{\Delta} \left. \frac{\partial \theta_c}{\partial \eta_c} \right|_{\eta_c=0} = -\frac{\beta}{\chi^{1/4}} \left. \frac{\partial \theta_F}{\partial \eta_F} \right|_{\eta_F=0} \quad (39)$$

to be solved with the conditions

$$\theta_F(\chi, \eta_F = 0) = \theta_c(\tilde{\chi}, \eta_c = 0) = \theta_w(\chi). \quad (40)$$

The second term on the left hand side of equation (39) denotes the heat transferred from the condensed fluid and the term on the right hand side, the heat transferred to the cooling fluid. The asymptotic solution of the problem for large values of α is important because it is applicable to many practical cases of metallic plates. For $\alpha \gg 1$ the nondimensional temperature of the plate changes very little in the longitudinal direction of the order of α^{-1} . Neglecting such a small quantity in first approximation, the temperature of the plate can be approximated by a unknown constant θ_{w0} . The thickness of the condensed phase, Δ , can be determined with the aid of equation (37) and the natural boundary layer flow is then self-similar, of the form

$$f_F = \theta_{w0}^{1/4} g(\theta_{w0}^{1/4} \eta_F, Pr_F) \quad \text{and} \quad \theta_F = \theta_{w0} \phi(\theta_{w0}^{1/4} \eta_F, Pr_F) \quad (41)$$

where $g(\xi, Pr_F)$ and $\phi(\xi, Pr_F)$ are the solutions of the classical problem

$$\frac{d^3 g}{d\xi^3} + \phi = \frac{1}{Pr_F} \left\{ \frac{1}{2} \left(\frac{dg}{d\xi} \right)^2 - \frac{3}{4} g \frac{d^2 g}{d\xi^2} \right\} \quad (42)$$

$$\frac{d^2 \phi}{d\xi^2} + \frac{3}{4} g \frac{d\phi}{d\xi} = 0 \quad (43)$$

$$g(0) = \left. \frac{dg}{d\xi} \right|_{\xi=0} = \phi(0) - 1 = 0,$$

$$\text{and } \left. \frac{dg}{d\xi} \right|_{\xi \rightarrow \infty} = \phi(\infty) = 0. \quad (44)$$

In these equations we used the invariance of the boundary layer equations (42) and (43), under the group of transformations $g \Rightarrow B^{1/4} g$, $\phi \Rightarrow B\phi$, and $\xi \Rightarrow B^{-1/4} \xi$, with B being arbitrary.

The solution of equations (42)–(44) can be found elsewhere [10]. In particular, the nondimensional temperature gradient at the wall is given by the very good correlation

$$\left. \frac{d\phi}{d\xi} \right|_{\xi=0} = -G(Pr_F) \approx -\frac{3}{4} \left[\frac{2Pr_F/5}{1 + 2Pr_F^{1/2} + 2Pr_F} \right]^{1/4}. \quad (45)$$

The unknown θ_{w0} can be found by using equations (41) and (45), to evaluate the right hand side of equation (39) and then integrating this equation over χ with the boundary conditions (21). On the other hand, the thickness of the condensed phase is obtained directly, replacing the calculated value of θ_{w0} in equation (37) and integrating this equation subject to the initial condition $\Delta_0(0) = 0$. The result is

$$\frac{(1 - \theta_{w0})^{3/4}}{(\theta_{w0})^{5/4}} = \beta G(Pr_F), \quad \Delta_0 = [(1 - \theta_{w0})\tilde{\chi}]^{1/4}. \quad (46)$$

The values of θ_{w0} can be obtained by solving this transcendental equation for given values of β and Pr_F . For large values of β , $\theta_{w0} \rightarrow 0$, $\Delta_0 \rightarrow \tilde{\chi}^{1/4}$, whereas $\theta_{w0} \rightarrow 1$, $\Delta_0 \rightarrow 0$ for small values of β . The first limit corresponds to the case where the thermal resistance of the natural boundary layer flow is negligible and the temperature of the plate is very close to T_∞ . This is the classical Nusselt's solution [6]. In the second case, we don't have a condensation process, because the temperature of the plate is very close to T_s leading to a conventional natural boundary layer flow. Once θ_{w0} and Δ_0 are known, the reduced Nusselt number, equation (36), can be evaluated, giving

$$Nu_c^* = \frac{(1 - \theta_{w0})^{3/4}}{\tilde{\chi}^{1/4}}. \quad (47)$$

This result can be improved by computing the next term in an expansion of the solution in powers of α^{-1} . Such a calculation is summarized in Appendix A and gives the correction factor

Table 1. Values of C_1 and θ_{w0} for different values of β (with $Pr_F = 1$, $G(1) = 0.4009218$)

β	θ_{w0}	C_1
0.5	0.901331	0.869698
1.0	0.797323	0.862092
2.5	0.587096	0.846103
5.0	0.415416	0.834886
10.0	0.272134	0.827513

$$[1 + \alpha^{-1} F(Pr, \beta, \chi)] + O(\alpha^{-2}) \quad (48)$$

for the reduced Nusselt number, equation (47), with F given by equation (A.12). The resulting approximation turns out to be very good even for α of order unity. From the local Nusselt number, we can obtain the overall number \overline{Nu} given by

$$\overline{Nu} = \int_0^1 Nu_c^* d\chi = \frac{4}{3} (1 - \theta_{w0})^{3/4} \times \left[1 + \frac{4(7/8 - C_1)}{7\alpha(1 - \theta_{w0})^{1/4}} + O(\alpha^{-2}) \right]. \quad (49)$$

The values of θ_{w0} and C_1 can be found in Table 1 for different values of the parameter β . Due to the fact that C_1 is always less than $7/8$, the \overline{Nu} increases with decreasing values of α .

4.2. Limit $\alpha/\varepsilon^2 \sim 1$ (thermally thick wall)

In this case the nondimensional temperature varies linearly across the plate between values $\theta_{wc}(\chi)$ and $\theta_{wF}(\chi)$ at both faces, with $\theta_{wc}(\chi) - \theta_{wF}(\chi) = O(1)$. Here, $\theta_{wc}(\chi)$ and $\theta_{wF}(\chi)$ represent the nondimensional temperatures of the wall at $z = 1/2$ and $z = -1/2$, respectively. In this limit, the longitudinal heat conduction can be neglected, except in small regions close to the edges of the plate. The heat flux from the condensed fluid to the right lateral face of the wall is equal locally to the heat flux from the left lateral face of the plate to the cooling fluid and equal to the heat flux across the solid at the same longitudinal position. The fact that the heat flux in the condensed phase is finite at the lower edge implies $[\theta_{wF}, \theta_F] \sim \chi^{1/5}$ for small χ . The regions around the edges where longitudinal conduction matters are now of length $O(\varepsilon)$, comparable to the thickness of the plate. The temperature of the solid in these regions differs from the temperature of the corresponding fluid by an order of $\varepsilon^{1/5}$.

In the limit, $\alpha/\varepsilon^2 \rightarrow 0$, most of the temperature drop occurs in the solid, that is $\theta_{wc} \rightarrow 1$ and $\theta_{wF} \rightarrow 0$, except in small regions near the edges. Outside of these regions, the variables are of the form

$$\theta_w = \frac{1}{2} - z + \left(\frac{\alpha}{\varepsilon^2} \right)^{4/5} \theta_{wF} + \left(\frac{\alpha}{\varepsilon^2} \right)^{4/3} \theta_{wc} + O \left[\left(\frac{\alpha}{\varepsilon^2} \right)^{8/5} \right] \quad (50)$$

$$\Delta = \left(\frac{\alpha}{\varepsilon^2}\right)^{1/3} \Delta_0 + O\left[\left(\frac{\alpha}{\varepsilon^2}\right)^{2/3}\right] \quad (51)$$

and

$$\begin{aligned} \tilde{f}_F &= \left(\frac{\alpha}{\varepsilon^2}\right)^{1/5} \tilde{g}\left[\left(\frac{\alpha}{\varepsilon^2}\right)^{1/5} \tilde{\eta}_F, Pr_F\right], \\ \tilde{\theta}_F &= \left(\frac{\alpha}{\varepsilon^2}\right)^{4/5} \tilde{\phi}\left[\left(\frac{\alpha}{\varepsilon^2}\right)^{1/5} \tilde{\eta}_F, Pr_F\right] \end{aligned} \quad (52)$$

where $\tilde{g}(\xi, Pr_F)$ and $\tilde{\phi}(\xi, Pr_F)$ are the solutions of the classical problem of a boundary layer with a constant heat flux at the wall ($d\tilde{\phi}/d\xi|_0 = -1$), which can be found elsewhere [10], with the variables $\tilde{\eta}_F$, \tilde{f}_F and $\tilde{\theta}_F$ defined as

$$\begin{aligned} \tilde{\eta}_F &= \frac{Ra^{1/4}(y-h/2)}{L\chi^{1/5}}, \\ \tilde{f}_F &= \frac{\psi_F}{\nu_F Ra^{1/4} \chi^{4/5}} \quad \text{and} \quad \tilde{\theta}_F = \theta_F / \chi^{1/5}. \end{aligned} \quad (53)$$

The solution to this problem can be written by the following correlation [10]

$$\tilde{\phi}(0, Pr_F) = \tilde{G}(Pr_F) = \left(\frac{4 + 9Pr_F^{1/2} + 10Pr_F}{Pr_F}\right)^{1/5}. \quad (54)$$

To this order, the nondimensional plate temperature and the nondimensional thickness are given by

$$\begin{aligned} \theta_w &\sim \frac{1}{2} - z + \left(\frac{\beta\alpha}{\varepsilon^2}\right)^{4/5} \tilde{G}(Pr_F) \chi^{1/5} \left(\frac{1}{2} + z\right) \\ &\quad - \left(\frac{\alpha}{\varepsilon^2}\right)^{4/5} (1-\chi)^{1/3} \left(\frac{1}{2} - z\right) \end{aligned} \quad (55)$$

$$\Delta \sim \left(\frac{\alpha}{\varepsilon^2}\right)^{1/3} \left[\frac{3}{4}(1-\chi)\right]^{1/3} + O[(\alpha/\varepsilon^2)^{2/3}]. \quad (56)$$

The local reduced Nusselt number is then given as

$$\begin{aligned} Nu_c^* &\sim \frac{\alpha}{\varepsilon^2} \left[1 - \left(\frac{\beta\alpha}{\varepsilon^2}\right)^{4/5} \tilde{G}(Pr_F) \chi^{1/5} \right. \\ &\quad \left. - \left(\frac{\alpha}{\varepsilon^2}\right)^{4/3} \left[\frac{3}{4}(1-\chi)\right]^{1/3} \right] \end{aligned} \quad (57)$$

while the overall Nusselt number is

$$\begin{aligned} \overline{Nu} &= \int_0^1 Nu_c^* d\chi \sim \frac{\alpha}{\varepsilon^2} \\ &\quad \times \left[1 - \frac{5}{6} \left(\frac{\beta\alpha}{\varepsilon^2}\right)^{4/5} \tilde{G}(Pr_F) - \left(\frac{3\alpha}{4\varepsilon^2}\right)^{4/3}\right]. \end{aligned} \quad (58)$$

5. COMPARISON BETWEEN ASYMPTOTIC AND NUMERICAL RESULTS

For values of α of order unity, the nondimensional governing equations can be integrated using Keller's method [12] for the boundary layer equations, together with the technique of alternate directions from Peaceman, Rachford and Douglas for the Laplace equation [13]. Due to the elliptic nature of the problem, the cooling fluid equations were solved initially using an arbitrary plate temperature profile, obtaining the corresponding heat flux distribution to be used for the solid energy equation. We use this flux as boundary conditions for the pseudo-transient heat conduction equation in the plate, giving the new plate temperature distribution after a small artificial time step, $\Delta\tau = 0.001$. The procedure continues until convergence is achieved. The mesh used for the cooling fluid balance equations was 50×90 , in the longitudinal and transversal directions, respectively. For the solid we used a 50×50 grid. We employed the values of $\varepsilon = 0.1$ and $Pr_F = 1$ for all computations.

In the limit of very large values of β , the temperature of the plate is practically uniform and close to the value of the temperature of the free natural stream, reducing the problem to the constant temperature case given by the classical Nusselt's solution. Here, the longitudinal heat conduction doesn't play an important role even for large values of α . For finite values of β , in the limit $\alpha \rightarrow 0$, the system of governing equations is singular and therefore it is necessary to include inner heat conducting layers at both edges of the plate. In particular, outside of these inner regions, there is an outer region where the longitudinal heat conduction through the plate is negligible in a first approximation. For different values of α , the corresponding values of the nondimensional temperature of the plate and the thickness of the condensate film, as a function of the longitudinal coordinate χ and $\beta = 1$, are shown in Figs. 2 and 3, obtained using numerical techniques. It is clear from Fig. 2 that for increasing values of the parameter α , the nondimensional temperature of the plate tends, asymptotically, to a specific uniform value $\theta_w \simeq 0.7973 \dots$, which depends on β (see Table 1).

For values of α much larger than 0.1 ($\alpha/\varepsilon^2 \gg 10$), the temperature at both surfaces of the plate are practically the same at each longitudinal position. This corresponds to the thermal thin wall regime. Otherwise, for values of α of the order of 0.1, there are noticeable transversal variations of temperature, indicating that the thermally thin wall approximation is no longer valid. For very small values of α , the temperature at the right surface of the plate tends to the saturated vapor temperature and similarly, the temperature at the left surface comes closer to that of the cooling fluid. This case corresponds to a process limited by the transversal heat conduction through the solid.

Figure 3 shows the numerical and asymptotic solutions for the nondimensional thickness of the con-

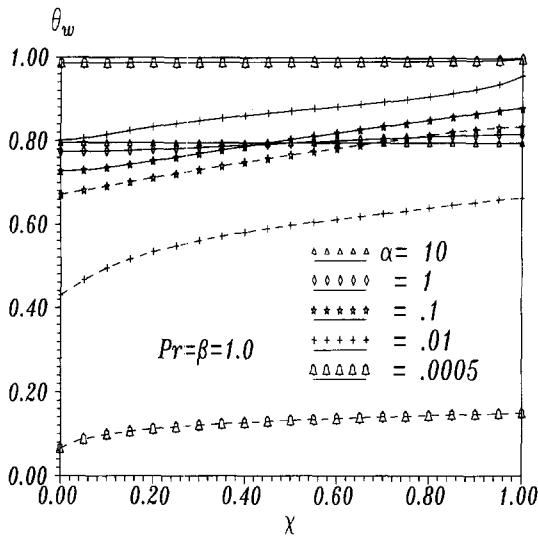


Fig. 2. Numerical nondimensional plate temperatures as a function of the longitudinal coordinate χ , for different values of α , $\beta = 1$ and $\varepsilon = 0.1$. For values of $\alpha \geq 1$ the temperature at both lateral surfaces of the plate is indistinguishable when using the plot scale.

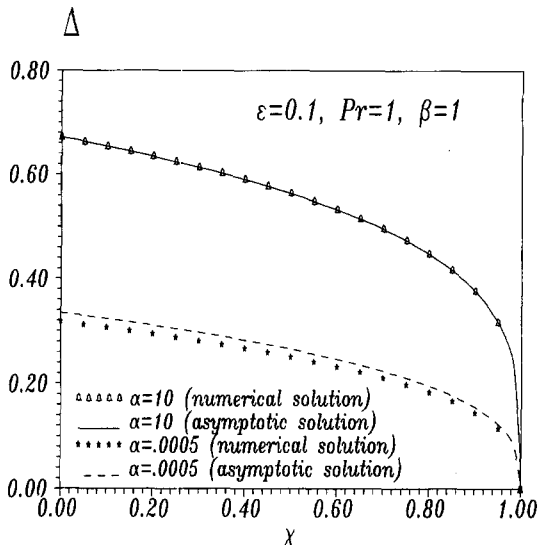


Fig. 3. Asymptotic and numerical nondimensional thicknesses as a function of the longitudinal coordinate χ , for high and low values of α , $\beta = 1$ and $\varepsilon = 0.1$.

densified fluid, as a function of the longitudinal coordinate for two very different values of α . For the higher value ($\alpha = 10$), the solution recovers the classical Nusselt's theory and there is a very good agreement between the numerical and asymptotic results. For the smaller value ($\alpha = 0.0005$), there is also a relatively good agreement by using the asymptotic solution for the thermally thick wall regime. The nondimensional thickness is strongly reduced by decreasing the value of α or α/ε^2 . Finally, Fig. 4 shows the numerical and asymptotic values of the overall Nusselt number \overline{Nu} as a function of α , for two different values of β . The influence of β on \overline{Nu} is very small for values of $\alpha \ll \varepsilon^2$.

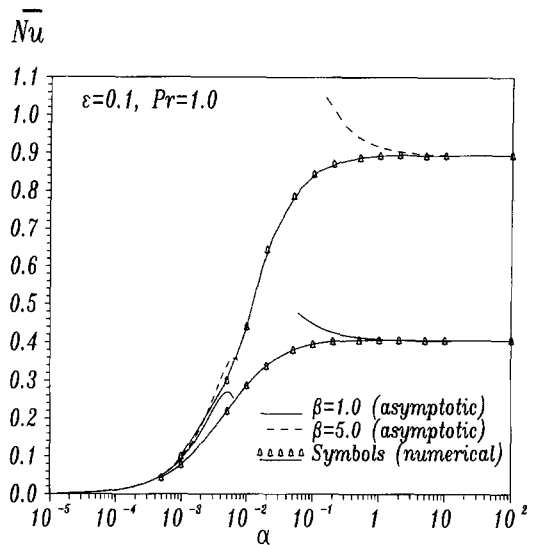


Fig. 4. Overall Nusselt number, \overline{Nu} , as a function of α for $\beta = 1, 5$ and $\varepsilon = 0.1$.

On the other hand, for very large values of α , the influence of β is now very strong, reaching the asymptotic values obtained in the thermally thin wall regime. A two term asymptotic solution for large values of β indicates that the overall Nusselt number increases as the value of α decreases. This would lead to the existence of the overall Nusselt number at a finite value of α . The numerical results show an imperceptible maximum for \overline{Nu} for each value of β within a few milliseals, compared with the asymptotic values for $\alpha \rightarrow \infty$, confirming the asymptotic behavior obtained using perturbation techniques for this limit, which indicates the existence of a maximum for a finite value of α .

6. CONCLUSIONS

In this paper, we studied the condensation process of a saturated vapor in contact with one lateral surface of a thin vertical plate. A natural cooling flow is assumed at the other lateral surface of the plate. The finite thermal conductivity of the plate material allows heat to transfer longitudinally through the plate, thus changing the mathematical character of the problem, from parabolic to elliptic. Assuming the plate to have adiabatic leading and trailing edges, the local heat natural convection through the lateral surface of the plate, affected strongly by the axial heat conduction, governs the spatial evolution of the plate temperature and the condensed layer thickness. The two asymptotic limits of large and small values of the parameter α , for different values of β , have been analyzed for this condensation process. In general, for large values of α , the plate temperature varies little in the longitudinal direction, thus producing a singular behavior for the Nusselt number close to the leading edge. As the value of α decreases, the plate temperature comes closer to

the temperature of the natural cooling flow, trying to reach this value if the values of β are sufficiently high.

Acknowledgements—This work has been supported by a grant from CONACyT, Mexico 4456-A.

REFERENCES

1. Patankar, S. V. and Sparrow, E. M., Condensation on an extended surface. *Journal of Heat Transfer*, 1979, **101**, 434–440.
2. Wilkins, J. E., Condensation on an extended surface. *Journal of Heat Transfer*, 1980, **102**, 186–187.
3. Sarma, P. K., Chary, S. P. and Dharma Rao, V., Condensation on a vertical plate fin of variable thickness. *International Journal of Heat and Mass Transfer*, 1988, **31**, 1941–1944.
4. Brouwers, H. J. H., Film condensation on non-isothermal vertical plates. *International Journal of Heat and Mass Transfer*, 1989, **32**, 655–663.
5. Méndez, F. and Treviño, C., Film condensation generated by a forced cooling fluid. *Journal of European Mechanics/Fluids*, 1996, **15**, 217–240.
6. Nusselt, W., Die Oberflächenkondensation des Wasserdampfes. *Zeitschrift des Vereins deutscher Ingenieure*, 1916, **60**, 541–546, 569–575.
7. Treviño, C. and Méndez, F., Transient conjugate condensation process on a vertical plate with finite thermal inertia. *International Journal of Heat and Mass Transfer*, 1996, **39**, 2221–2230.
8. Incropera, F. P. and DeWitt, D. P., *Fundamentals of Heat and Mass Transfer*, 3rd edn. Wiley, New York, 1990, p. 589.
9. Wetzler, H., *Kennzahlen der Verfahrenstechnik*. Hüthig, Heidelberg, 1985.
10. Kays, W. M. and Crawford, M. E., *Convective Heat and Mass Transfer*, 2nd edn. McGraw-Hill, New York, 1980.
11. Burmeister, L. C., *Convective Heat Transfer*. Wiley, New York, 1983, p. 490.
12. Cebeci, T. and Bradshaw, P., *Physical and Computational Aspects of Convective Heat Transfer*. Springer, Berlin, 1984.
13. Sod, A. G., *Numerical Methods in Fluid Dynamics: Initial and Initial Boundary-Value Problems*. Cambridge University Press, U.S.A., 1985.
14. Córdova, J. and Treviño C., Effects of longitudinal heat conduction of a vertical thin plate in a natural convective cooling process. *Wärme- und Stoffübertragung*, 1994, **29**, 195–204.

APPENDIX A

The solution of equations (21), (29)–(33), (35), (37) and (39) for $\alpha \gg 1$ can be obtained using a perturbation series of the form

$$\theta_w = \sum_{j=0}^{\infty} \frac{1}{\alpha^j} \theta_{wj}(\chi) \quad \theta_F = \sum_{j=0}^{\infty} \frac{1}{\alpha^j} \theta_{Fj}(\chi, \eta_F)$$

$$f_F = \sum_{j=0}^{\infty} \frac{1}{\alpha^j} f_{Fj}(\chi, \eta_F) \quad \text{and} \quad \Delta = \sum_{j=0}^{\infty} \frac{1}{\alpha^j} \Delta_j(\chi, \eta_F) \quad (\text{A1})$$

where the leading terms are given by equations (41) and (46). In this Appendix we carry out the analysis up to the first order.

Introducing equations (41) and (A1) into equations (39) and (37), collecting terms of order α^{-1} , integrating twice the resulting energy equation along χ and integrating once the evolution equation of the thickness of the condensed phase, we obtain θ_{w1} and Δ_1 as

$$\theta_{w1} = \frac{16}{21} (1 - \theta_{w0})^{3/4} \left(\chi^{7/4} - (1 - \chi)^{7/4} - \frac{7}{4} \chi + C_1 \right)$$

$$= \frac{16}{21} (1 - \theta_{w0})^{3/4} \left(\chi^{7/4} + C_1 - 1 - \sum_{n=2}^{\infty} a_n \chi^n \right)$$

$$\Delta_1 = \frac{4}{21} \left\{ \frac{[\frac{4}{11} (1 - \chi)^{11/4} - \frac{7}{8} (1 - \chi)^2 + \frac{45}{88}]}{\chi^{3/4}} + \frac{4}{11} \chi^2 - C_1 \chi^{1/4} \right\} \quad (\text{A2})$$

where C_1 is an unknown constant to be found from the second-order equations. For convenience, we have written θ_{w1} as power series of χ (obviously, θ_{w1} can also be written in terms of $\tilde{\chi}$, remembering that $\tilde{\chi} = 1 - \chi$). Here a_n are the coefficients of the binomial expansion of $(1 - \chi)^{7/4}$. Substituting equation (A1) into equations (29)–(33) and collecting terms proportional to α^{-1} , the quantities θ_{F1} and f_{F1} , satisfy a linear problem whose solution for a surface temperature of the form $\theta_{w1} = A\chi^n$ would be

$$f_{F1} = A\chi^n \theta_{w0}^{-3/4} g_1[\theta_{w0}^{1/4} \eta_F, Pr_F], \quad \theta_{F1} = A\chi^n \phi_1[\theta_{w0}^{1/4} \eta_F, Pr_F] \quad (\text{A3})$$

with $g_1(\xi, Pr_F)$ and $\phi_1(\xi, Pr_F)$ satisfying the following linear equations

$$\frac{d^3 g_1}{d\xi^3} + \phi_1 + \frac{1}{Pr_F} \left\{ -\frac{dg_1}{d\xi} \frac{dg_1}{d\xi} + \frac{3}{4} \frac{d^2 g}{d\xi^2} g_1 + \frac{3}{4} g \frac{d^2 g_1}{d\xi^2} - n \left[\frac{dg}{d\xi} \frac{dg_1}{d\xi} - \frac{d^2 g}{d\xi^2} g_1 \right] \right\} = 0 \quad (\text{A4})$$

$$\frac{d^2 \phi_1}{d\xi^2} + \frac{3}{4} g \frac{d\phi_1}{d\xi} + \frac{3}{4} \frac{d\phi}{d\xi} g_1 - n \left[\frac{dg}{d\xi} \phi_1 - \frac{d\phi}{d\xi} g_1 \right] = 0 \quad (\text{A5})$$

$$g_1 = \frac{dg_1}{d\xi} = \phi_1 - 1 = 0 \quad \text{at } \xi = 0$$

$$\text{and} \quad \frac{dg_1}{d\xi} = \phi_1 = 0 \quad \text{for } \xi \rightarrow \infty. \quad (\text{A6})$$

The functions $G_1(n, Pr_F) \equiv -d\phi_1/d\xi|_{\xi=0}$ obtained from the solution of equations (A4)–(A6) are given in ref. [14].

Then, taking advantage of equation (A3) and of the series expansions (A2) for θ_{w1} and Δ_1 , and applying the superposition principle to the linear problem for f_{F1} and θ_{F1} , we immediately obtain

$$\frac{\partial \theta_{F1}}{\partial \eta} \Big|_{\eta=0} = -\frac{16}{21} (1 - \theta_{w0}) \left((C_1 - 1) G_1(0, Pr_F) + G_1 \left(\frac{7}{4}, Pr_F \right) \chi^{7/4} - \sum_{n=2}^{\infty} a_n G_1(n, Pr_F) \chi^n \right) \quad (\text{A7})$$

and

$$\frac{1}{\Delta} \frac{\partial \theta_{F1}}{\partial \eta} \Big|_{\eta=0} = \frac{1 - \theta_w}{\Delta}$$

$$= -\frac{16}{21} (1 - \theta_{w0})^{1/2} \left(\chi^{7/4} (1 - \chi)^{-1/4} - \frac{7}{4} \chi (1 - \chi)^{-1/4} - (1 - \chi)^{3/2} + C_1 (1 - \chi)^{-1/4} \right). \quad (\text{A8})$$

Finally

$$C_1 = \frac{H_N(Pr_F, \beta)}{H_D(Pr_F, \beta)} \quad (\text{A9})$$

is obtained by carrying equations (A7) and (A8) into equation (39) and integrating this equation over χ with the boundary conditions (21). Here,

$$H_N = \frac{7}{8} + \frac{4}{3}\beta(1-\theta_{w0})^{1/2} \left[G_1(0) - \frac{3}{10}G_1\left(\frac{7}{4}\right) + \sum_{n=2}^N \frac{a_n G_1(n)}{(\frac{4}{3}n+1)} \right] \quad (\text{A10})$$

$$H_D = 1 + \frac{4}{3}\beta G_1(0)(1-\theta_{w0})^{1/2} \quad (\text{A11})$$

where we used the notation $G_1(n) = G_1(n, Pr_F)$.

The factor $F(Pr_F, \beta, \chi)$ in the correction, equation (48), to the reduced Nusselt number, equation (47), can now be evaluated as

$$F = \frac{16}{21} \frac{1}{(1-\theta_{w0})^{1/4}} \left[1 - \frac{3}{4}C_1 - \chi^{7/4} - \frac{(1-\chi)^{7/4}}{11} - \frac{\frac{\chi^{11/4}}{11} - \frac{7\chi^2}{32} + \frac{45}{352}}{(1-\chi)} + \sum_{n=2}^N a_n \chi^n \right] \quad (\text{A12})$$